JOURNAL OF SOLID STATE CHEMISTRY 50, 41–50 (1983)

A New Analysis of the Fluorescence Spectrum of Eu^{3+} in *A*-Type La_2O_3

O. K. MOUNE, P. PORCHER, AND P. CARO

Laboratoire des Elements de Transition dans les Solides, ER 210 du CNRS
1, Place Aristide Briand, 92190 Meudon Bellevue, France

Received April 12, 1983; in revised form June 27, 1983

The fluorescence spectrum of Eu^{3+} doping the *A*-type sesquioxide La_2O_3 has been reinterpreted using dye laser excitation of the $^5D_0$ level. New assignments and crystal field parameters are obtained. The E representation of the $^7F_1$ level appears to be clearly split at 77 K. From this fact and the general broadness of the lines at 300 K, one suggests that the doping Eu^{3+} ion is slightly off-center with respect to the theoretical lanthanum coordinates and may tunnel between different off-center positions at high temperature.

The fluorescence spectrum of Eu^{3+} doping at low concentration the hexagonal sesquioxide A-La_2O_3 has been previously interpreted (*1*). In the course of a study of two of the crystallographic forms of the oxycarbonates $(LaO)_2CO_3$ doped with europium, a spectrum for Eu^{3+} ions engaged within an impurity in the samples was obtained as the result of scanning the dye laser excitation (*2*). This spectrum excited at 5810.2 Å (17,211 cm^{-1}) at 300 K was very similar, but had some definite differences, with the one to be expected from the excitation into the $^5D_0$ level of Eu^{3+} doping A-La_2O_3 according to the sequence of energy levels reported in Ref. (*1*). As A-La_2O_3 is a very likely impurity for the oxycarbonates the parasite spectrum was checked against the one of a 1% Eu^{3+} doped sample of pure A-La_2O_3 prepared by firing the oxalate in a platinum crucible at 1200°C for 24 hr. The sample being cooled was kept under an atmosphere free of water and carbon dioxide. The fluorescence spectrum of this material, excited at 5810.2 Å, was identical to the one for the impurity in the oxycarbonates, whereas the fluorescence spectrum excited under conventional uv light (3600 Å) was in fact identical to the original one (*1*) as obtained by Linarès and Gaume-Mahn (*3*). It was then apparent that a few misinterpretations had occurred concerning the fluorescence lines originating from the $^5D_0$ level in Ref. (*1*). In 1973 dye laser excitation was not available and consequently the attributions to $^5D_0$ cannot be checked. However, an important consequence is that the site symmetry to be attributed to the doping Eu^{3+} atom cannot be with confidence ascribed to C_{3v} in agreement with the theoretical site symmetry of the lanthanum atom in the cristallographic structure.

I. The Fluorescence Spectrum of Eu^{3+} in A-La_2O_3

The fluorescence spectrum of A-$La_2O_3:Eu^{3+}$ was obtained at 300, 77, and 4.2 K in the wavelength range 4500–7000 Å through a 1-m Jarrel–Ash monochromator

0022-4596/83 $3.00

(Fig. 1). The fluorescence was excited with a uv high pressure mercury lamp, equipped with a Wood filter (≃3600 Å). The data are very rich, since at 77 K more than 120 lines are recorded, due to the ^5D_J ($J = 0, 1, 2, 3$) $\rightarrow$ ^7F_J ($J = 0, 1, 2, 3, 4, 5, 6$) transitions (Table I). Such a spectrum is difficult to interpret completely, since many transitions occurring from different emitting levels are superimposed. To help the attributions, we measured the spectrum with two Eu^{3+} concentrations (1 and 5%). This fact, as well as the temperature, modifies the emitting levels quenching and the relative intensities of the transitions. An alternative help was the use of the rhodamine 6G dye laser selective excitation, accorded on the $^5D_0 \rightarrow {}^7F_0$ transition. This last technique is most powerful, since it is easy to attribute unambiguously the ^7F_J Stark levels giving an allowed transition from $^5D_0$. The only remaining problem was the hypersensitive $^5D_0 \rightarrow {}^7F_2$ transition, accompanied by various vibronic lines as well as $^5D_2 \rightarrow {}^7F_2$. But a comparison with another transition, say, $^5D_1 \rightarrow {}^7F_2$, magnetic dipolar and nonhypersensitive, gave the $^7F_2$ Stark level sequence. Moreover, the comparison of $^5D_2 \rightarrow {}^7F_5$ with $^5D_1 \rightarrow {}^7F_5$ at different temperatures gave a quite complete $^7F_5$ Stark level sequence, as well as some of their associated irreducible representations.

The differences with the interpretation in Ref. (*1*) are as follows:

(a) Instead of a single line at 16,772 cm^{-1} for the $^5D_0(A_1) \rightarrow {}^7F_1(E)$ transition, the dye laser showed two lines at 16,791 and 16,766 cm^{-1}. These lines show up as well in the uv excitation. The first one was attributed by the authors of Ref. (*1*) to a line from $^5D_2$.

(b) The lines at 15,929 and 15,871 cm^{-1} which, according to the table in (*1*), correspond to transitions $^5D_1 \rightarrow {}^7F_4$ remain under selective excitation of $^5D_0$. They apparently are vibronic satellites of $^5D_0 \rightarrow {}^7F_2$.

(c) The line predicted from (*1*) at 15,171 cm^{-1} as member of the $^5D_0 \rightarrow {}^7F_3$ group is in fact a $^5D_1 \rightarrow {}^7F_5$ transition, but we detected a new line at 15,269 cm^{-1} which belongs to $^5D_0 \rightarrow {}^7F_3$.

(d) The lines predicted from (*1*) at 14,503 and 14,312 cm^{-1} as $^5D_0 \rightarrow {}^7F_4$ are not observed under dye laser excitation. Instead, a strong line appears at 14,128 cm^{-1} as part of the $^5D_0 \rightarrow {}^7F_4$ group. This line was taken by the authors of Ref. (*1*) as a spurious mercury line (*3*). The levels derived from the present analysis are given in Table II.

II. Energy Level Sequence and Crystal Field Parameters

In our study, one of the most surprising fact is the observation of a degeneracy lifting of the E, C_{3v} irreducible representation for the $^7F_1$ level (Table II). The splitting of 25 cm^{-1} is observed for all the recorded transitions having $^7F_1$ as final level, i.e., $^5D_0 \rightarrow {}^7F_1$, $^5D_1 \rightarrow {}^7F_1$, and $^5D_2 \rightarrow {}^7F_1$. Except for these cases, the number of observed lines is in agreement with the C_{3v} point site selection rules for all other transitions. It seems difficult to explain such a feature. For instance, because of the quite perfect homothetic ratio we shall expect a 6-cm^{-1} splitting for the corresponding $^5D_1$ irreducible representation. We did not measure any such splitting, however, and the other E (C_{3v}) levels remain degenerate as well.

We tried to simulate the data by computing crystal field parameters (cfp) in the 49 × 49 $|SLJM_J\rangle$ basis of the ^7F_J (*4*). The first step was to consider a pure C_{3v} point symmetry for the rare earth. Five cfp are then involved. From our experimental energy level scheme, we found $B^2_0 = -668 \pm 16$ cm^{-1}, $B^4_0 = 448 \pm 33$ cm^{-1}, $B^4_3 = 1216 \pm 16$ cm^{-1}, $B^6_0 = 1041 \pm 23$ cm^{-1}, $B^6_3 = -231 \pm 16$ cm^{-1}, and $B^6_6 = 558 \pm 19$ cm^{-1}, all levels being quite correctly simulated since the rms deviation is 8.3 cm^{-1}. Naturally, the sixth rank cfp differ from those of Ref. (*1*) as a consequence of a different attribution

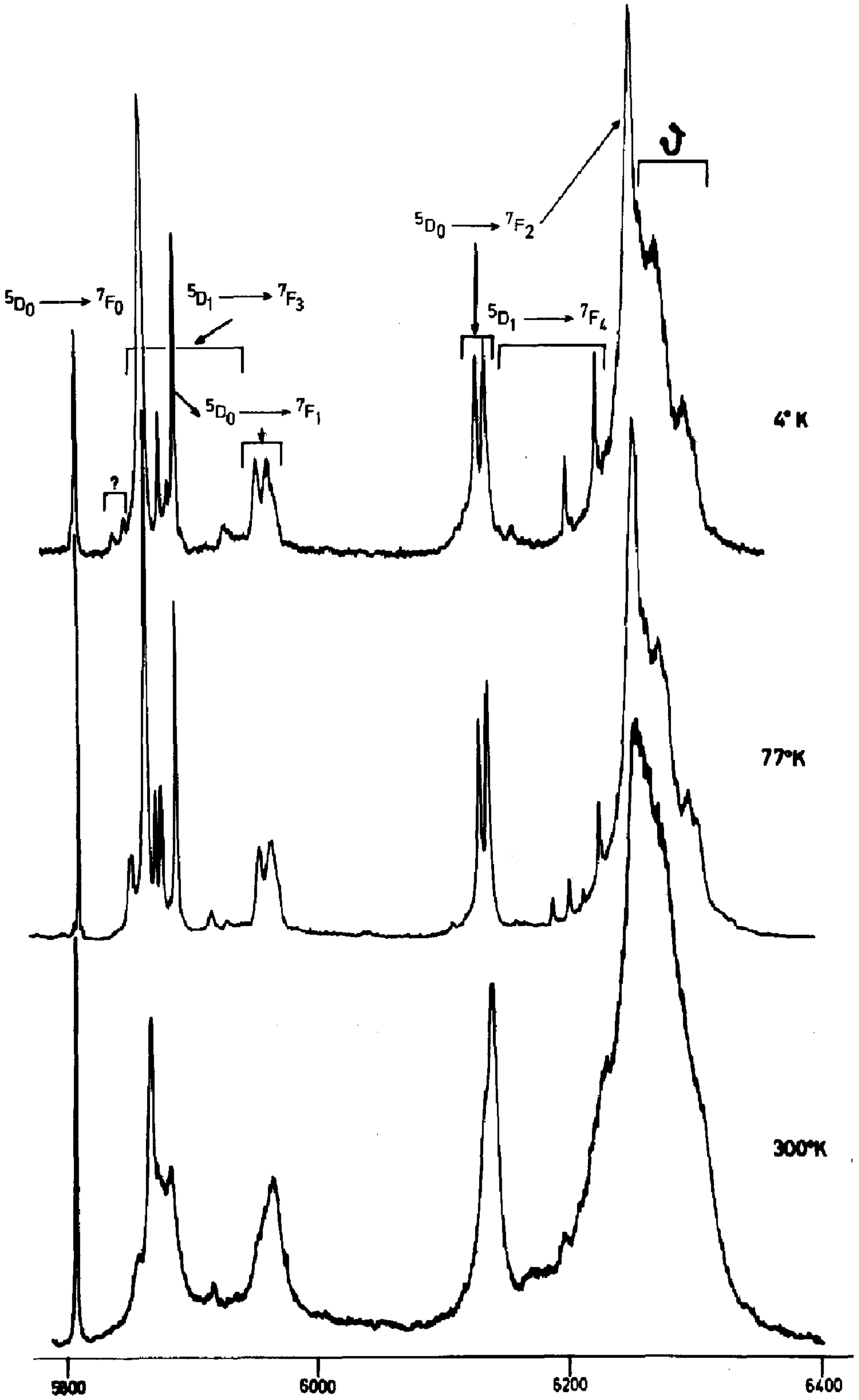

FIG. 1. Emission spectra of Eu^{3+} : La$_2$O$_3$ (1%) at 4, 77, and 300 K under uv excitation (v = vibronics).

for $^7F_4$ Stark levels. The second step was to take into account the degeneracy lifting in $^7F_1$, by adding to the crystal field Hamiltonian another operator involving the B_2^2 parameter. Then the site is considered to have no symmetry (27 parameters in all), but only the C_{3v} parameters and the B_2^2 have nonzero values. Results from the adjustment were $B_0^2 = -665 \pm 16$ cm^{-1}, $B_2^2 = 50$ cm^{-1} (fixed), $B_0^4 = 471 \pm 36$ cm^{-1}, $B_3^4 = 1221$

TABLE I

OBSERVED EMISSION LINES AND ASSIGNMENT FOR Eu^{3+} : La_2O_3 (1%) AT 77 AND 4 K UNDER UV EXCITATION

E (cm^{-1})			Assignment	E (cm^{-1})			Assignment
77 K	4 K	Transition	(C_{3v})	77 K	4 K	Transition	(C_{3v})
21,636	21,635	$^5D_3 \rightarrow {}^7F_4$	$A_1 \rightarrow A_1$	19,461	19,458	$^5D_2 \rightarrow {}^7F_3$	$E \rightarrow A_2$
21,503		$^5D_3 \rightarrow {}^7F_4$	$? \rightarrow E$		19,444	v	
21,473		$^5D_2 \rightarrow {}^7F_0$	$E \rightarrow A_1$	19,440	19,439	$^5D_2 \rightarrow {}^7F_3$	$E \rightarrow E$
21,455		$^5D_2 \rightarrow {}^7F_0$	$A_1 \rightarrow A_1$	19,427	19,423	$^5D_2 \rightarrow {}^7F_3$	$E \rightarrow A_1$
21,424	21,422	$^5D_3 \rightarrow {}^7F_4$	$A_1 \rightarrow E$	19,309		v	
21,400		$^5D_3 \rightarrow {}^7F_4$	$? \rightarrow A_1$	19,305	19,303	$^5D_2 \rightarrow {}^7F_3$	$E \rightarrow A_2$
21,386	21,382	$^5D_2 \rightarrow {}^7F_0$	$E \rightarrow A_1$		19,296	v	
21,367		$^5D_2 \rightarrow {}^7F_4$	$E \rightarrow A_1$	18,980		$^5D_1 \rightarrow {}^7F_0$	$E \rightarrow A_1$
21,304		$^5D_3 \rightarrow {}^7F_4$	$? \rightarrow A_1$	18,946	18,942	$^5D_1 \rightarrow {}^7F_0$	$A_2 \rightarrow A_1$
21,267		$^5D_3 \rightarrow {}^7F_4$	$? \rightarrow E$	18,859		$^5D_2 \rightarrow {}^7F_4$	$E \rightarrow A_1$
21,241		$^5D_3 \rightarrow {}^7F_4$	$? \rightarrow E$	18,843		$^5D_2 \rightarrow {}^7F_4$	$A_1 \rightarrow A_1$
21,234	21,230	$^5D_3 \rightarrow {}^7F_4$	$A_1 \rightarrow E$	18,772	18,770	$^5D_2 \rightarrow {}^7F_4$	$E \rightarrow A_1$
21,225		$^5D_2 \rightarrow {}^7F_1$	$A_1 \rightarrow A_2$	18,749		$^5D_1 \rightarrow {}^7F_1$	$E \rightarrow A_2$
21,205		?			18,690	v	
21,184	21,180	$^5D_3 \rightarrow {}^7F_4$	$A_1 \rightarrow E$		18,697	v	
21,156	21,151	$^5D_2 \rightarrow {}^7F_1$	$E \rightarrow A_2$	18,696	18,711	$^5D_1 \rightarrow {}^7F_1$	$A_2 \rightarrow A_2$
21,033		$^5D_2 \rightarrow {}^7F_1$	$A_1 \rightarrow E$		18,721	v	
21,013		$^5D_2 \rightarrow {}^7F_1$	$A_1 \rightarrow E$		18,730	v	
20,963	20,958	$^5D_2 \rightarrow {}^7F_1$	$E \rightarrow E$	18,679		?	
20,939	20,932	$^5D_2 \rightarrow {}^7F_1$	$E \rightarrow E$	18,644		$^5D_2 \rightarrow {}^7F_4$	$E \rightarrow E$
20,565		$^5D_3 \rightarrow {}^7F_5$	?	18,628		$^5D_2 \rightarrow {}^7F_4$	$A_1 \rightarrow E$
20,549		$^5D_2 \rightarrow {}^7F_2$	$A_1 \rightarrow A_1$		18,604	?	
20,533		$^5D_2 \rightarrow {}^7F_2$	$A_1 \rightarrow E$	18,580		$^5D_2 \rightarrow {}^7F_4$	$E \rightarrow A_2$
20,524		$^5D_3 \rightarrow {}^7F_5$	?	18,558	18,556	$^5D_2 \rightarrow {}^7F_4$	$E \rightarrow E$
20,481	20,478	$^5D_2 \rightarrow {}^7F_2$	$E \rightarrow A_1$	18,533	18,521	$^5D_1 \rightarrow {}^7F_1$	$A_2 \rightarrow E$
20,462	20,458	$^5D_2 \rightarrow {}^7F_2$	$E \rightarrow E$	18,495	18,492	$^5D_1 \rightarrow {}^7F_1$	$A_2 \rightarrow E$
20,351	20,349	$^5D_3 \rightarrow {}^7F_5$	?		18,477	?	
20,220		$^5D_2 \rightarrow {}^7F_2$	$A_1 \rightarrow E$	18,433		$^5D_2 \rightarrow {}^7F_4$	$A_1 \rightarrow A_1$
20,155	20,153	$^5D_2 \rightarrow {}^7F_2$	$E \rightarrow E$		18,423	?	
20,136	20,149	v[a]		18,415		$^5D_2 \rightarrow {}^7F_4$	$E \rightarrow E$
20,103	20,131	v		18,387		$^5D_2 \rightarrow {}^7F_4$	$E \rightarrow E$
20,088	20,095	v					$A_1 \rightarrow E$
20,041	20,035	v		18,362	18,360	$^5D_2 \rightarrow {}^7F_4$	$E \rightarrow A_1$
20,027		v		18,320		$^5D_2 \rightarrow {}^7F_4$	$E \rightarrow E$
19,586		$^5D_2 \rightarrow {}^7F_3$	$E \rightarrow E$	18,298	18,296	$^5D_2 \rightarrow {}^7F_4$	$E \rightarrow E$
19,570		$^5D_2 \rightarrow {}^7F_3$	$A_1 \rightarrow E$	18,072		$^5D_1 \rightarrow {}^7F_2$	$E \rightarrow A_1$
	19,552	?		18,054		$^5D_1 \rightarrow {}^7F_2$	$E \rightarrow E$
	19,535	?		18,036	18,035	$^5D_1 \rightarrow {}^7F_2$	$A_2 \rightarrow A_1$
19,527		$^5D_2 \rightarrow {}^7F_3$	$A_1 \rightarrow A_2$	18,020	18,017	$^5D_1 \rightarrow {}^7F_2$	$A_2 \rightarrow E$
19,511			$A_1 \rightarrow E$		17,951	?	
19,500	19,499	$^5D_2 \rightarrow {}^7F_3$	$E \rightarrow E$	17,742		$^5D_1 \rightarrow {}^7F_2$	$E \rightarrow E$

TABLE I—*Continued*

E (cm^{-1})			Assignment
77 K	4 K	Transition	(C_{3v})
17,710		$^5D_1 \rightarrow {}^7F_2$	$A_2 \rightarrow E$
17,699		$^5D_2 \rightarrow {}^7F_5$	$E \rightarrow E$
17,658		$^5D_2 \rightarrow {}^7F_5$	$E \rightarrow A_1$
17,642		$^5D_2 \rightarrow {}^7F_5$	$A_1 \rightarrow A_1$
17,613		$^5D_2 \rightarrow {}^7F_5$	$E \rightarrow E$
17,570		$^5D_2 \rightarrow {}^7F_5$	$E \rightarrow A_1$
17,547		$^5D_2 \rightarrow {}^7F_5$	$A_1 \rightarrow A_2$
			$E \rightarrow E$
17,481		$^5D_2 \rightarrow {}^7F_5$	$E \rightarrow A_2$
17,461		$^5D_2 \rightarrow {}^7F_5$	$E \rightarrow E$
17,376		$^5D_2 \rightarrow {}^7F_5$	$E \rightarrow E$
17,313		$^5D_2 \rightarrow {}^7F_5$	$A_1 \rightarrow E$
			$E \rightarrow A_2$
17,248		$^5D_2 \rightarrow {}^7F_5$	$E \rightarrow E$
17,224	17,221	v	
17,210	17,209	$^5D_0 \rightarrow {}^7F_0$	$A_1 \rightarrow A_1$
17,206	17,203	v	
	17,120	?	
	17,095	?	
17,090		$^5D_1 \rightarrow {}^7F_3$	$E \rightarrow E$
17,057	17,055	$^5D_1 \rightarrow {}^7F_3$	$A_2 \rightarrow E$
17,050		$^5D_1 \rightarrow {}^7F_3$	$E \rightarrow A_2$
17,031		$^5D_1 \rightarrow {}^7F_3$	$E \rightarrow E$
17,018	17,015	$^5D_1 \rightarrow {}^7F_3$	$A_2 \rightarrow A_2$
16,997	16,995	$^5D_1 \rightarrow {}^7F_3$	$A_2 \rightarrow E$
16,984	16,977	$^5D_0 \rightarrow {}^7F_1$	$A_2 \rightarrow A_2$
		$^5D_1 \rightarrow {}^7F_3$	$A_2 \rightarrow A_1$
16,900		$^5D_1 \rightarrow {}^7F_3$	$E \rightarrow A_2$
16,869	16,869	$^5D_1 \rightarrow {}^7F_3$	$A_2 \rightarrow A_2$
16,793	16,788	$^5D_0 \rightarrow {}^7F_1$	$A_1 \rightarrow E$
16,766	16,763	$^5D_0 \rightarrow {}^7F_1$	$A_1 \rightarrow E$
16,362		$^5D_1 \rightarrow {}^7F_4$	$E \rightarrow A_1$
16,303	16,301	$^5D_0 \rightarrow {}^7F_2$	$A_1 \rightarrow A_1$
16,285	16,283	$^5D_0 \rightarrow {}^7F_2$	$A_1 \rightarrow E$
16,226	16,224	?	
16,148		$^5D_1 \rightarrow {}^7F_4$	$E \rightarrow E$
16,114	16,112	$^5D_1 \rightarrow {}^7F_4$	$A_2 \rightarrow E$
16,085		$^5D_1 \rightarrow {}^7F_4$	$E \rightarrow A_2$
16,050	16,048	$^5D_1 \rightarrow {}^7F_4$	$A_2 \rightarrow A_2$
15,978	16,973	$^5D_0 \rightarrow {}^7F_2$	$A_1 \rightarrow E$
15,956	16,952	v	
15,927	16,924	v	
15,892		v	
15,862	18,866	v	
15,849		v	
15,323	16,325	$^5D_0 \rightarrow {}^7F_3$	$A_1 \rightarrow E$
15,282	16,280	$^5D_0 \rightarrow {}^7F_3$	$A_1 \rightarrow A_2$
15,264	16,262	$^5D_0 \rightarrow {}^7F_3$	$A_1 \rightarrow E$
15,252	16,248	$^5D_0 \rightarrow {}^7F_3$	$A_1 \rightarrow A_1$
15,205		$^5D_1 \rightarrow {}^7F_5$	$E \rightarrow E$
15,171	15,167	$^5D_1 \rightarrow {}^7F_5$	$A_2 \rightarrow E$
15,075		$^5D_1 \rightarrow {}^7F_5$	$E \rightarrow A_2$
15,039	15,035	$^5D_1 \rightarrow {}^7F_5$	$A_2 \rightarrow A_2$
15,020	15,015	$^5D_1 \rightarrow {}^7F_5$	$A_2 \rightarrow E$
14,998		?	
14,980		$^5D_1 \rightarrow {}^7F_5$	$E \rightarrow E$
	14,947	$^5D_1 \rightarrow {}^7F_5$	$A_2 \rightarrow E$
14,919		?	
14,845		$^5D_1 \rightarrow {}^7F_5$	$E \rightarrow E$
14,812	14,808	$^5D_1 \rightarrow {}^7F_5$	$A_2 \rightarrow E$
14,779	14,774	$^5D_1 \rightarrow {}^7F_5$	$A_2 \rightarrow A_2$
	14,612	?	
14,596	14,596	$^5D_0 \rightarrow {}^7F_4$	$A_1 \rightarrow A_1$
14,380	14,380	$^5D_0 \rightarrow {}^7F_4$	$A_1 \rightarrow E$
14,184	14,182	$^5D_0 \rightarrow {}^7F_4$	$A_1 \rightarrow A_1$
14,140	14,136	$^5D_0 \rightarrow {}^7F_4$	$A_1 \rightarrow E$
14,119	14,118	$^5D_0 \rightarrow {}^7F_4$	$A_1 \rightarrow E$

[a] v: vibronics.

± 17 cm^{-1}, $B_0^6 = 1045 \pm 24$ cm^{-1}, $B_3^6 = -232 \pm 17$ cm^{-1}, $B_6^6 = 554 \pm 20$ cm^{-1}. The rms deviation was 8.5 cm^{-1}, almost the same as previously. The list of computed and experimental levels is given in Table II. It can be seen that, with the exception of $^7F_1$, the computed splitting of the C_{3v}, E representation is rather small, always less than 10 cm^{-1}. However, such splittings are not experimentally observed.

III. Optical Study of Part of the La$_2$O$_3$–Eu$_2$O$_3$ Binary System

Because of the difference in ionic radii between lanthanum and europium one may suspect that the smaller europium atom distorts the lanthanum site and that the optical signal is the indication that europium does not fit well into the (LaO)$_n^{n+}$ framework in the *A*-type structure (*5*). Moreover it is

TABLE II

CALCULATED AND EXPERIMENTAL ENERGY LEVELS OF Eu^{3+} : La_2O_3 (1%) (SEE TEXT FOR VALUES OF THE CRYSTAL FIELD PARAMETERS)

		Cal.		Exp.		
	Irreducible representation (C_{3v})	(1) (C_{3v})	(2) (No symmetry)	Selective excitation λE(17,210 cm^{-1})	uv excitation	
				77 K	77 K	4 K
$^7F_0$	A_1	0	0	0	0	0
$^7F_1$	A_2	231	232	228	226	232
	E	430	417	419	417	421
			442	444	444	446
$^7F_2$	A_1	919	917	908	907	908
	E	925	920	925	925	926
			931			
	E	1225	1223	1232	1232	1236
			1228			
$^7F_3$	E	1892	1890	1886	1882	1884
			1894			
	A_2	1928	1927	1927	1928	1929
	E	1940	1935	1946	1946	1947
			1944			
	A_1	1955	1956	1958	1958	1961
	A_2	2079	2078		2077	2079
$^7F_4$	A_1	2616	2616	2614	2614	2613
	E	2839	2836	2829	2830	2829
			2840			
	A_2	2888	2888		2891	2894
	A_1	3031	3031	3026	3026	3027
	E	3065	3063	3069	3070	3073
			3067			
	E	3080	3079	3088	3091	3091
			3082			
$^7F_5$	E	3773	3772	3775		
			3773			
	A_1	3788	3787	3813		
	A_2	3905	3904	3907		
	E	3917	3916	3927		
			3919			
	E	4088	4005	3999		
			4009			
	E	4144	4140	4134		
			4148			
	A_2	4169	4168	4168		
$^5D_0$	A_1			17,210	17,210	17,209
$^5D_1$	A_2				18,946	18,942
	E				18,980	
$^5D_2$	E				21,386	21,382
	A_1				21,455	
	E				21,473	
$^5D_3$					24,240	24,240
					24,319	
					24,420	

known that small amounts of yttric impurities in the *A*-type structure induce monoclinic *B*-type Ln_2O_3 domains, presumably because of mechanical stresses similar to those which can be readily produced by thermal pulse-annealing in thin A-type oxide films (*6*). The *B*-type domains are easily detected from optical experiments, for example, on yttrium-doped neodymium oxide (*7*).

To test the influence of the europium concentration on the stability of the *A*-type lanthanum oxide structure, we prepared compositions within the La_2O_3–Eu_2O_3 binary system and recorded the fluorescence spectra of the samples. The binary phase diagrams of the lanthanum oxide with the other rare earth oxide have been established by Foëx and his co-workers (*8, 9*) with the exception of europium (because of the volatility at high temperatures). The phase diagrams established through thermal analysis and high temperature X rays show a rather large domain of *A*-type stability at temperatures above 1400°C which shall extend at this temperature up to 30% or more Eu_2O_3 according to the diagrams for Sm and Gd. We prepared our samples in the same conditions as described above, i.e., at 1200°C for 24 hr. The fluorescence spectra under uv excitation at 77 K for several compositions are shown in Fig. 2.

The lines broaden as the europium concentration increases, which is to be expected for solid solutions, and the relative intensity of the emissions from the $^5D_1$ level strongly decreases (concentration quenching); but the position of the $^5D_0 \rightarrow {}^7F_0$ transition and the splitting of $^5D_0 \rightarrow {}^7F_1$ are not greatly affected by the increase in europium concentration up to 25% molar within the *A*-type solid solution domain. With more Eu_2O_3 the spectrum changes to one characteristic of a *B*-type solid solution with structural disorder superimposed on signals from the three different cristallographic sites for the europium atom (*10*).

IV. Discussion

The space group of the A-type rare earth sesquioxide structure has been the subject of disputes in the past. The differences were reviewed by Aldebert and Traverse (*11*). It is now generally agreed from neutron diffraction (*11, 12*), electron diffraction (*13*), and Raman spectroscopy (*14*) that the correct space group is $P\bar{3}m1$, in agreement with Pauling's original suggestion (*15*). In fact all of the models considered have in common the existence of a trigonal cristallographic axis.

To understand the lifting of the degeneracy of the E (C_{3v}) representation in $^7F_1$ it is necessary to assume that the threefold symmetry is destroyed at the europium site. This is either a local phenomenon or one should admit the improbable fact that the established space group of the *A*-type structure is incorrect.

To get some quantitative insight into the crystallographic distortions needed to produce the observed spectrum, we simulated (*16*), by an electrostatic calculation, the change induced in the crystal field parameters by a small displacement of the europium atom, destroying the threefold symmetry. We displaced the europium atom in the (0001) plane in the $[1\bar{1}00]$ direction in order to tilt the C_3 axis of the site by 1°. The distortion chosen is a step towards the formation of the B-type site in the *A*-type structure. In those conditions the europium atom is off-center with respect to the normal lanthanum atom site by 0.042 Å. The calculation was done with point charges only (*17*). In the conventional *A*-type structure the computed B_0^2 value is $-2108\ \mathrm{cm}^{-1}$. In the distorted structure it is $-2051\ \mathrm{cm}^{-1}$ but a B_2^2 of 280 cm^{-1} is created. The C_{3v} parameters of ranks 4 and 6 are practically unchanged by the 1° distortion, and the numerous other parameters induced are very small. Taking the ratio of B_q^2 exp/B_q^2 calc. = 0.32 as a correction factor for the effective

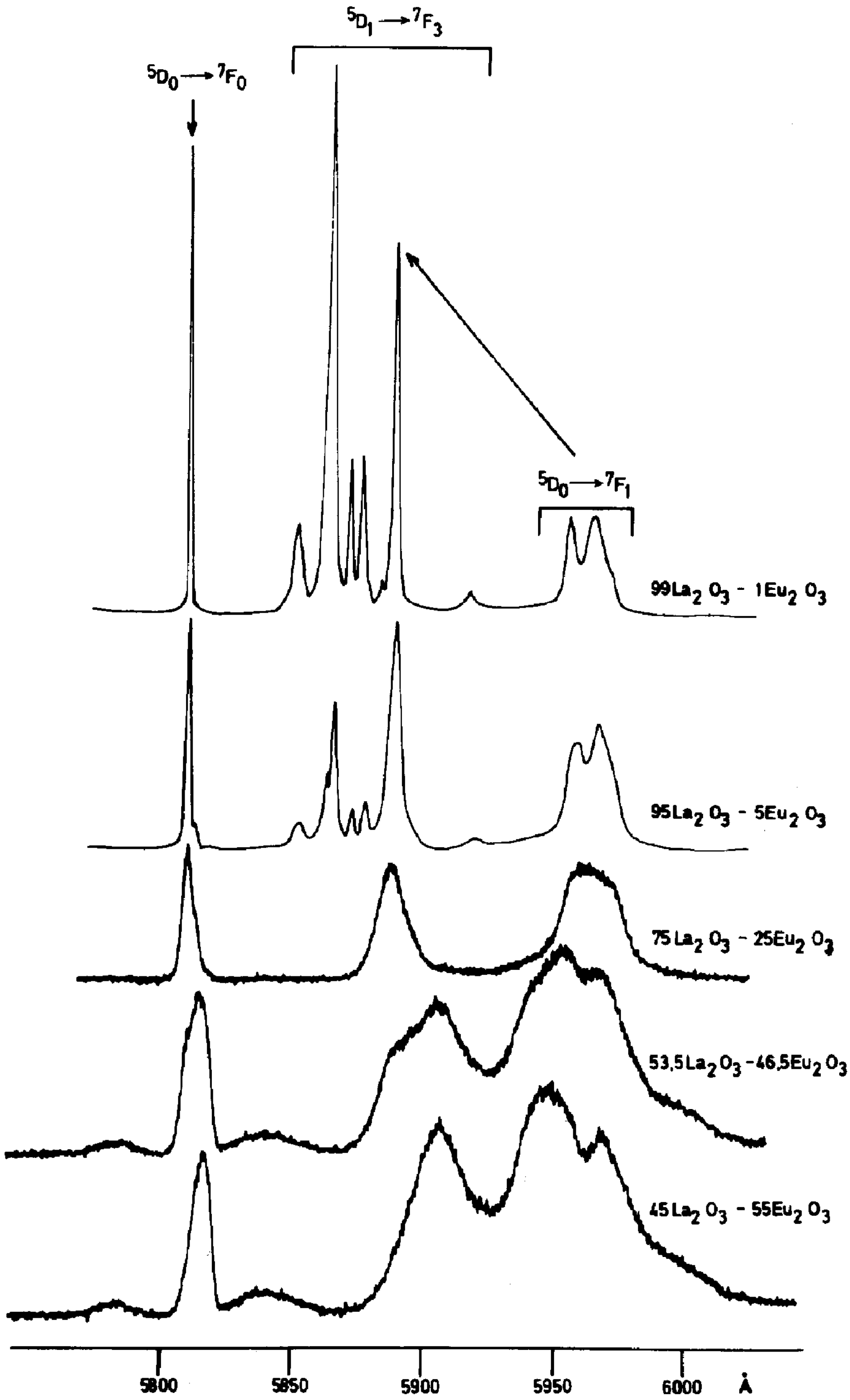

FIG. 2. Emission spectra of compositions in the Eu_2O_3–La_2O_3 binary diagram under uv excitation at 77 K.

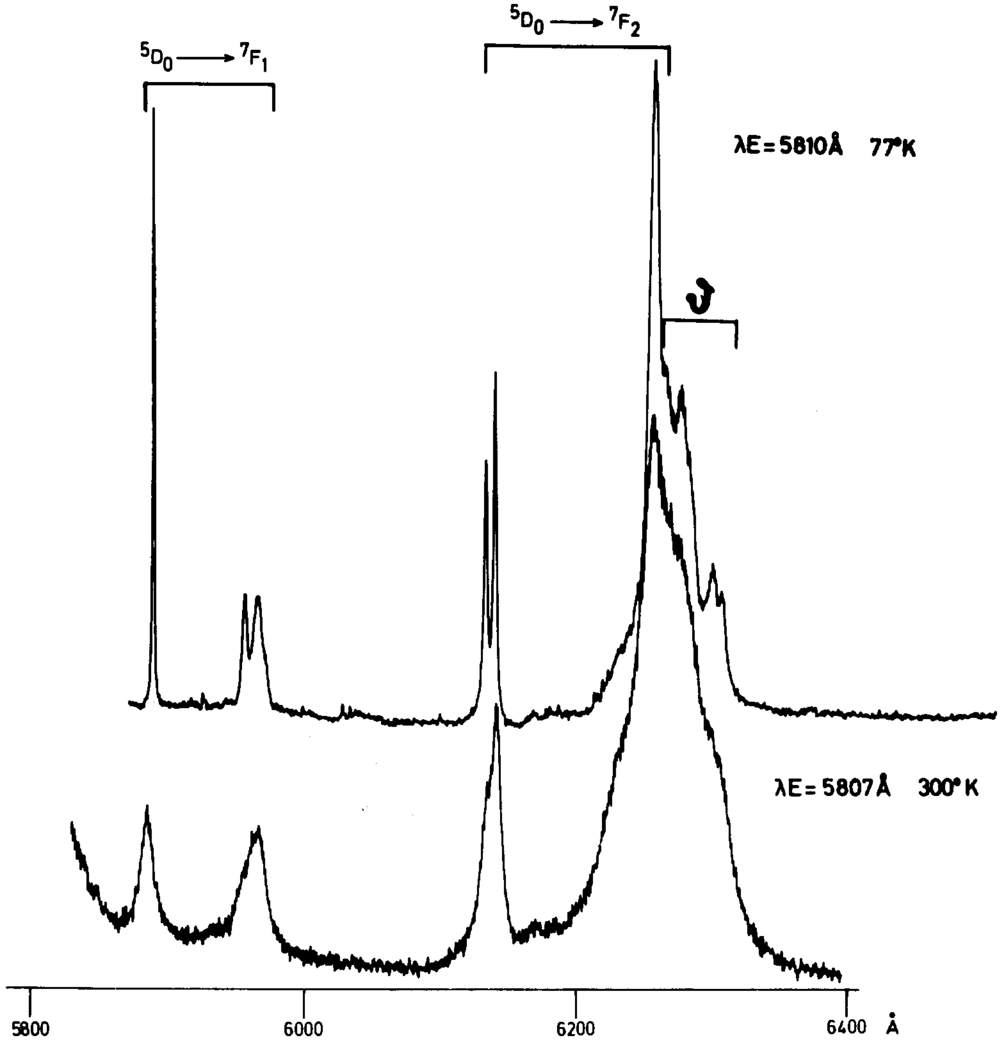

FIG. 3. Dye laser excitation (λ_E) at 77 and 300 K of the emission spectrum of Eu^{3+} : La_2O_3 (1%) (ν = vibronics).

Slater radial integrals (*17*) the induced effective B_2^2 parameter for that distortion should be 88 cm^{-1}. The experimental value being 50 cm^{-1}, the tilt angle sufficient to generate the observed result will be roughly 30 min of an arc.

It is clear then that the degeneracy lifting of the E representation of $^7F_1$ comes from a very small crystallographic distortion, and is seen only because the particular electrostatic arrangement of the atoms involved yields high values for B_2^2 when it is disturbed.

But other interpretations, such as electron–phonon coupling (*18–20*), could explain why only the $^7F_1$ E level is split. On the other hand, the fact that at 300 K the splitting observed at 77 K has disappeared within the broadening of the lines (Fig. 3) may indicate a phenomenon similar to what happens by doping a structure like $KTaO_3$ with lithium (*21–23*); at 77 K the doping

Eu^{3+} element could be off-center with respect to the ideal lanthanum position.

The phenomenon reported here, whatever its explanation, needs more investigation especially on single crystals which can be grown but which are mechanically fragile because of their lamellar structure, and are also very sensitive to moisture and carbon dioxide.

References

1. C. Linarès and F. Gaume-Mahn, *C.R. Acad. Sci. Paris* **277,** 431 (1973).
2. O. K. Moune-Minn and P. Caro, *J. Cryst. Spectrosc. Res.* **12,** 157 (1981).
3. C. Linarès and F. Gaume-Mahn, personal communication, 1981.
4. P. Porcher and P. Caro, *J. Chem. Phys.* **65,** 89 (1976).
5. P. Caro, *J. Less-Common Met.* **16,** 367 (1968).
6. C. Boulesteix, P. Caro, M. Gasgnier, C. Henry la Blanchetais, and G. Schiffmacher, *Phys. Lett. A* **34,** 437 (1971).
7. P. Caro, M. Faucher, J. Derouet, and M. G. Alves, *Rev. Chim. Miner.* **10,** 317 (1973).
8. J. Coutures, A. Rouanet, R. Vergés, and M. Foëx, *J. Solid State Chem.* **17,** 171 (1976).
9. J. Coutures, F. Sibieude, and M. Foëx, *J. Solid State Chem.* **17,** 377 (1976).
10. J. Dexpert-Ghys, M. Faucher, and P. Caro, *Phys. Rev. B* **23,** 607 (1981).
11. P. Aldebert and J. P. Traverse, *Mater. Res. Bull.* **14,** 303 (1979).
12. J. X. Boucherle and J. Schweizer, *Acta Crystallogr. Sect. B* **31,** 2745 (1975).
13. O. Greis, *J. Solid State Chem.* **34,** 39 (1980).
14. J. H. Denning and S. D. Ross, *J. Phys. C* **5,** 1123 (1972).
15. L. Pauling, *Z. Kristallogr.* **70,** 187 (1929).
16. Courtesy of Mrs. M. Faucher.
17. M. Faucher, J. Dexpert-Ghys, and P. Caro, *Phys. Rev. B* **21,** 3689 (1980).
18. J. Zarembowitch, J. Gouteron, and A. M. Lejus, *Phys. Status Solidi B* **94,** 249 (1979).
19. J. Gouteron, D. Michel, A. M., Lejus, and J. Zarembowitch, *J. Solid State Chem.* **38,** 288 (1981).
20. S. I. Boldish and W. B. White, *Spectrochim. Acta Part A* **35,** 1235 (1979).
21. J. J. Van der Klink, D. Rytz, F. Borsa, and V. T. Hochli, *Phys. Rev. B* **27,** 89 (1983).
22. Y. Yacoby and S. Just, *Solid State Commun.* **15,** 715 (1974).
23. F. Borsa and U. T. Hochli, *Phys. Rev. Lett.* **45,** 1884 (1980).